Discrimination of isomeric trisaccharides and their relative quantification in honeys using trapped ion mobility spectrometry

Cédric Przybylski, Véronique Bonnet

Discrimination of isomeric trisaccharides and their relative quantification in honeys using Trapped Ion Mobility Spectrometry

Cédric Przybylski*[†] and Véronique Bonnet [‡]

[†] Sorbonne Université, CNRS, Institut Parisien de Chimie Moléculaire, IPCM, 4 Place Jussieu, 75005 Paris, France.

E-mail: cedric.przybylski@sorbonne-universite.fr

[‡] Université de Picardie Jules Verne, Laboratoire de Glycochimie, des Antimicrobiens et des Agroressources, LG2A, CNRS UMR 7378, 33 rue Saint Leu, 80039 Amiens, France.

ABSTRACT

Carbohydrates play a myriad of critical roles as key intermediaries for energy storage, cell wall constituents, or also fuel for organisms. The deciphering of multiple structural isomers based on the monosaccharides composition (stereoisomers), the type of glycosidic linkages (connectivity) and the anomeric configuration (α and β), remains a major analytical challenging task. The possibility to discriminate 13 underivatized isomeric trisaccharides were reported using electrospray ionization coupled to trapped ion mobility spectrometry (ESI-TIMS). After optimization of scan ratio enhancing both the mobility resolving power (R) and resolution (r), fingerprints from 5 different honeys were obtained. Seven trisaccharides with relative content varying from 1.5 to 58.3%, were identified. It was demonstrated that their relative content and/or their ratio could be used to ascertain origin of the honeys. Moreover, such direct approach constitutes an alternative tool to current longer chromatographic runs, paving the way to a transfer as suitable routine analysis.

Keywords (6 max): ion-mobility, carbohydrates, trisaccharides, honey, ESI-TIMS, collision cross section.

1. INTRODUCTION

Carbohydrates or glycans are ubiquitous and the most abundant biological polymers in nature occurring in many important biological processes (Varki, 2015). Their role and function are beyond key biological intermediary for energy storage and fuel for organisms. Indeed, they can, for example, serve as building blocks for synthesis of higher macromolecules (nucleotides, glycoproteins, …) or by modulating the molecular recognition in many physio-pathological processes (Marth, 2008; Varki, 2015). Moreover, they are also the most rapidly evolving class of biomolecules through the evolution. Although it motivates numerous efforts for their characterization, their structural deciphering remains a critical bottleneck. Indeed, carbohydrates sequencing poses a major analytical challenge due to their inherent structural diversity, which is subject to a pressing need emphasized by national research councils (EGSF and IBCarb Network & European Science Foundation, 2014; National Research Council (US), 2012). Such complexity is mainly due to:

i) monosaccharides composition i.e. the carbohydrate based building blocks which are often stereoisomers that differ only in their stereochemistry at one particular carbon atom (glucose (Glc); galactose (Gal); mannose (Man)…).

ii) type of glycosidic linkages (connectivity) established between backbones of two building blocks, leading to linear or branched structures with diverse regioisomers.

iii) anomeric configuration (α and β), relative to the stereogenic centre appearing consecutively to a glycosidic bond formation. As example, considering a sequence of three monomers, more than 1.13×10^7 trisaccharides can be theoretically obtained (Laine, 1994). Historically, NMR is the reference method to determine the configurational information of carbohydrates, but require mg scale amounts, and allows only relative detection limit of ≈3-5%, restricting the identification

of small amounts of coexisting isomers (Duus et al., 2000). Mass spectrometry (MS) is also very used to identify and elucidate carbohydrates sequence, since it accurately and rapidly measure a mass-to-charge ratio (*m/z*), with sub-µg requirement, but intrinsic limit arising for stereoisomers discrimination ability (Dell & Morris, 2001). Further information can be also extracted regarding connectivity and so on sequence can be obtained using MS and iterative fragmentation (Ashline et al., 2007; Carroll et al., 1995; Riggs et al., 2018; Schindler et al., 2017). Nevertheless, as regards isomers, most of time very similar fragmentation pathways are obtained, impairing rigorous discrimination. Liquid chromatography (LC) with or without coupling to MS represents an alternative way for configurational isomers differentiation, but can be restricted by resolving power to track one given isomer within potential others in complex mixture (Lareau et al., 2015). In addition, derivatization step is very often a mandatory condition (Hofmann et al., 2015; Hofmann & Pagel, 2017). Recent IR or UV spectroscopies coupled to MS have proved their usefulness to obtain fingerprinting and delineate some anomeric forms (Ben Faleh et al., 2019; Mucha et al., 2017; Riggs et al., 2018; Schindler et al., 2018; Gray et al., 2017). A promising approach named ion mobility-MS (IM-MS) has been recently introduced and could overcome aforementioned limitations. IM-MS is a 2D method, which has potentiality to resolve glycan isomers (Clowers et al., 2005; Hofmann & Pagel, 2017; Zheng et al., 2017). Practically, their corresponding ions are separated not only according to their *m/z*, but also as function of their size and shape in the gas phase, thanks to the conversion of mobility into a collision cross section (CCS). IM-MS has been successfully applied to the characterization of large variety of derivatized or underivatized carbohydrates using travelling wave ion mobility (TWIM) (Harvey et al., 2018; Clowers et al., 2005; Paglia et al., 2014). Hofmann et al. (2015) have elegantly demonstrated that six pentylaminated disaccharides can be differentiated according to their stereochemistry, con-

nectivity and anomeric configuration, but also that a relative anomeric content can be estimated until 0.1%. Other IM technologies such as field asymmetric ion mobility spectrometry (FAIMS) or drift tube ion mobility spectrometry (DTIMS) was also investigated for glycan analysis (Gabryelski & Froese, 2003; Clowers et al., 2005; Gaye et al., 2015; Paglia et al., 2014; Xie et al., 2020). Nonetheless, resolution of isomeric glycans by IM sometimes still fails to address particular cases. Hence, the quest of improving IM separation efficiency remains one of the most challenging field in IM-MS glycan analysis. To fulfil this objective, different strategies have been deployed such as screening of various metal adduction (Huang & Dodds, 2013, 2015; Xie et al., 2020; Zheng, Zhang, et al., 2017), or the formation of diastereomeric adducts (Gaye et al., 2016) or the development of more resolving instruments. In this sense, Nagy et al. (2018) have tailored serpentine ion pathway, and McKenna et al. (2019) have developed a cyclic TWIM allowing multipass separations. Recently, trapped ion mobility spectrometry (TIMS) was introduced by Bruker. TIMS was notably successfully applied for the analysis of glycosaminoglycan (Wei et al., 2019) as well as to permethylated lacto-*N*-tetrasaccharides (Pu et al., 2016). In the present work, we report efforts to discriminate 13 isomeric trisaccharides (Figure S1) without any derivatization using electrospray ionization-TIMS (ESI-TIMS). The ability of the newly TimsTOF™ instrument to differentiate studied carbohydrates according to their structures and shapes was investigated. Moreover, usefulness of approach was validated as regards some criteria such as an unambiguous identification, rapid analysis, relative quantification features of trisaccharides in five honeys. We therefore propose the use of our TIMS strategy to extract glycan distribution to serve as characteristic fingerprint applicable in several field such as foodstuff samples quality control, which remains a major challenge.

2. MATERIALS AND METHODS

2.1. Standard Trisaccharides. D-cellotriose (≥95%) and inulotriose (≥90%), was purchased from Megazyme (Berkshire, UK). Erlose (≥ 95%), laminaritriose (≥95%), D-gentianose (≥97%), 1,4-β- D-mannotriose (≥95%) and 4'galactosyllactose (≥95%) were purchased from Carbosynth (Berkshire, UK). Maltotriose hydrate (≥95%), isomaltotriose (≥98%), D-panose (≥97%), D-(+)-melezitose monohydrate (≥99.0%), D-(+)-raffinose pentahydrate (≥98.0%), 1-kestose (≥98.0%) were purchased from Sigma Aldrich (Saint-Quentin Fallavier, France).

2.2 Solvents. Methanol used for sample preparation was of LC grade and was purchased from VWR (West Chester, PA, USA). Water was of ultrapure quality.

2.3 Samples

2.3.1 Solutions. Stock solutions were made at 10 mM in water and then diluted to 10 µM in methanol/water (1:1 v/v).

2.3.2 Honeys. 5 different honeys (3 from artisanal origin i.e. french lavender, rosemary and acacia acquired directly from beekeepers and 2 from industrial source i.e. forest, eucalyptus).

All honeys are purchased from different regions of France such as Provence (french lavender and rosemary), Alpine region (acacia), Auvergne region (forest) and Vosges mountains (eucalyptus).

Samples were prepared at 2% (w/v) in methanol/water (1:1 v/v), then further diluted by 1:2000 in the same solvent and passed through a 0.22 µm filter to remove particulate matter, homogenized by mechanical stirring and transferred to vials.

2.4 GC-MS analyses. Carbohydrate content in honey was controlled using the method described by Sanz *et al.* (Sanz, M.L., Sanz, J., & Martínez-Castro, I. (2004). See Supporting Information for further details.

2.5 TimsTOF™ Experiments. We used ESI-timsTOF™ (Bruker, Billerica, MA) operating with oTOF control v5.0 software. The source temperature was hold at 200°C, and the drying and nebulizing gas (N_2) operate at a flow rate of 3 L. min^{-1} and at a pressure of 0.3 bar, respectively. The instrument was calibrated using Tuning Mix G24221 (Agilent Technologies, Les Ulis, France). Applied voltages were +4 kV and -0.5 kV for capillary and endplate offset, respectively. Acquisition was achieved in the *m/z* 50-3000 range with a center at *m/z* 200. TIMS separation depends on the gas flow velocity (v_g), elution voltage ($V_{elution}$), ramp time (t_{ramp}), base voltage (V_{out}) and the electric field $(\vec{E})$. The reduced mobility, K_0, can be calculated as follows :

$$K_0 = \frac{v_g}{\vec{E}} = \frac{A}{(V_{elution} - V_{out})} \quad \text{(Eq. 1)}$$

The mobility calibration constant A was determined using known reduced mobilities of tuning mix components. The resolving power (R) and resolution (r) are defined as $R = (1/K_0)/w$ and $r = 1.18 \times [(1/K_0)_2 - (1/K_0)_1]/(w_1 + w_2)$, where w is the full peak width at half-maximum. To improve separation efficiency, scan rate ($Sr = \Delta V_{ramp}/t_{ramp}$) was tuned thank to imeX™ technology. For this, t_{ramp} is automatically set as function of manually adjusted ΔV_{ramp}. N_2 was used as buffer gas at funnel temperature (T = 305 K) with v_g set by the pressure difference of 0.169 mbar. A potential of 350 Vpp was applied to radially confine the trapped ion cloud. The measured inverse reduced mobilities were converted into collision cross sections (CCS) using the Mason-Schamp equation:

$$\Omega = \frac{(18\pi)^{1/2}}{16} \times \frac{q}{(k_B \times T)^{1/2}} \times \left[\frac{1}{m_i} + \frac{1}{m_g}\right]^{1/2} \times \frac{1}{N} \times \frac{1}{K_0} \quad \text{(Eq. 2)}$$

where q is the ion charge, k_B is the Boltzmann constant, N is the gas number density, m_i is the ion mass, and m_g is the gas molecule mass. TIMS-MS spectra and mobilograms were analyzed using Compass Data Analysis 5.1 (Bruker).

2.6 ESI-TIMS-MS analysis of the trisaccharides.

Throughout this study, isomeric trisaccharides were analysed in the positive ion mode as singly charged ions without any salt doping at *m/z* 505.176, 522.203, 527.158 and 543.132 for proton, ammonium, sodium and potassium adducts, respectively. Separation occurred according to their mobility. All samples was continuously infused at 5 µL.min^{-1} via a 250 mL syringe.

2.7 Theoretical Collision Cross Section Calculations.

All initial geometry relaxations were performed using the Merck molecular force field (MMFF94) implemented in Avogadro (v1.2). Geometry optimization was finalized using density functional theory (DFT) calculations with NWChem (v7.0). Theoretical CCS calculations were carried out in IMoS (v.1.1) using the average of ten trajectory method processes (Larriba & Hogan, 2013).

2.8 Data analysis.

Statistical tests and Principal component analysis (PCA) were performed using Origin Pro 2016 (OriginLab Corporation, MA, USA.)

3. RESULTS AND DISCUSSION

3.1 Ion mobility and collision cross sections determination of the library of trisaccharides.

As observed elsewhere the type of adducts exhibits different dependencies upon the identity of the bound cation, influencing the measured ion mobility (Huang & Dodds, 2013, 2015; Zheng, Zhang, et al., 2017). Nevertheless, for a given trisaccharide, the ion mobility did not necessarily increase/decrease proportionally according to the protonated form or ionic radii of the alkali

metal adduct as 154 pm, 99 pm, 137 pm and 151 pm for Na^+, K^+ and NH_4^+, respectively. Most importantly, it clearly appeared that the size of the adduct was not the only factor affecting the ion mobility, since it can be a hypothesised that each carbohydrate can adopt a preferred -most stable- conformation, which can be either close or distinct according to a given cation. As reported in Table 1, type of adduct can affect results at two level: (i) By supporting a straightforward identification. The mobility of two trisaccharide isomers, e.g. isomaltoriose and raffinose, cannot be discriminated using protonated forms (both with $1/K_0$ = 1.000 V.s/cm^2) but unambiguously distinguished via ammoniated ($1/K_0$ = 1.034 versus 1.001 V.s/cm^2, respectively), sodiated ($1/K_0$ = 1.033/0.984 versus 1.020 V.s/cm^2, respectively), or potassied adduct ($1/K_0$ =1.040/0.988 versus 1.027 V.s/cm^2, respectively). In this case, an increase in the size of the alkali metal ion allowed the two isomers to assume conformations which were more readily distinguished by mobility. (ii) By revealing other potential forms of trisaccharide such as epimers, connectivity isomers or more simply other conformations due to distinct adduction sites. The mobility of two forms for a given trisaccharide, e.g. sodiated and potassied 4'galactosyllactose yields to one and two peaks detected by ion mobility ($1/K_0$ = 0.990 versus 1.006 and 1.018 V.s/cm^2, respectively). Moreover, after thorough examination of the various values summarized in table 1, and except potential traces of maltotriose in isomaltoriose sample, as revealed by potassium adduct ($1/K_0$ = 1.041 versus 1.040 V.s/cm^2, respectively), none standard trisaccharide seems to contain residual presence of other one investigated in the herein study. One of the most emblematic features of ion mobility hold in its ability to discriminate isomeric forms even with subtle variation. To explore the potential of timsTOF™ as regards such aforementioned aim, results on four trisaccharides namely maltotriose,

Table 1. Recapitulative of the inverse reduced mobility of the 13 studied trisaccharides under various adducted forms at a scan rate of 5.5 V/ms and deducted collision cross section.

Name	Adduct	$1/K_0$ ($V.s.cm^{-2}$)	$^{TIMS}CCS_{N_2}$ (Å^2)	
			Experimental*	Theoretical
Maltotriose	H	1.000	205.8	205.9±3.7
	NH_4	1.006	206.8	206.7±4.1
	Na	1.038	213.3	214.2±6.2
	K	1.052/1.041	216.0/213.8	216.4±4.8
Isomaltotriose	H	0.997	205.2	205.0±4.8
	NH_4	1.034	212.6	212.6±2.8
	Na	1.033/0.984	212.3/202.1	212.8±4.8
	K	1.040/0.988	213.5/203.0	213.5±3.3
Raffinose	H	0.997	205.2	205.3±2.7
	NH_4	1.001	206.1	206.4±3.8
	Na	1.020	209.5	210.6±5.6
	K	1.027	211.0	211.3±3.8
Melezitose	H	0.999	205.5	205.4±2.9
	NH_4	1.003	206.3	206.2±4.2
	Na	0.982	201.8	202.4±3.2
	K	0.986	202.6	203.2±3.1
1-Kestose	H	0.995	204.7	204.6±3.9
	NH_4	1.013	208.3	208.2±2.9
	Na	0.999	205.5	206.7±5.2
	K	1.009	207.1	207.5±4.5
Gentianose	H	1.003	206.3	206.5±4.7
	NH_4	1.036	213.0	213.4±4.3
	Na	1.016/0.985	208.7/202.4	208.0±6.1
	K	1.030/1.004	211.6/206.2	211.3±2.4
Panose	H	0.995	204.7	204.6±4.4
	NH_4	1.007	207.0	206.8±3.5
	Na	1.018/1.025/0.981	209.2/210.7/201.6	209.3±7.0
	K	1.005/1.032	206.3/211.9	206.5±3.9
Cellotriose	H	1.021/1.070	210.2/220.1	210.4±3.7
	NH_4	1.042	214.1	214.3±3.3
	Na	1.041/1.023	213.9/210.2	213.7±5.9
	K	1.048	215.2	214.9±3.4
Laminatriose	H	1.021/1.073	210.1/220.7	210.1±4.2
	NH_4	1.062	218.3	218.3±4.5
	Na	1.029	211.5	211.3±5.6
	K	1.043/0.982	214.1/201.7	214.0±3.4
Mannotriose	H	1.040	213.9	213.9 ±3.9
	NH_4	1.039	213.6	213.5 ±3.8
	Na	1.028	211.4	212.0±5.2
	K	1.041	213.7	214.0±2.1
4'galactosyllactose	H	0.998/1.014	205.3/208.5	20509±4.1
	NH_4	0.995/1.014	204.6/208.7	204.7±4.6
	Na	0.990	203.5	203.7±6.2
	K	1.006/1.018	206.6/209.1	206.9±3.6
Inulotriose	H	1.053	216.7	216.8±2.8
	NH_4	1.045	214.7	214.9±3.3
	Na	0.992	203.9	203.9±5.9
	K	0.986/1.004	202.6/206.3	202.9±3.2
Erlose	H	0.991	203.9	204.6±3.6
	NH_4	0.990	203.4	203.8±3.6
	Na	1.007	206.9	208.4±5.1
	K	0.990	203.3	203.5±4.2

* Standard deviation was 0.4 Å^2.

isomaltotriose, cellotriose and mannotriose under the various adducts were compared. Such choice was motivated by differences in: i) connectivity, with isomaltotriose/maltotriose (α-D-Glc (1→6)/α-D-Glc (1→4), ii) anomery, with maltotriose/cellotriose (α-D-Glc (1→4)/(β- D-Glc(1→4)) and iii) composition, with cellotriose/ mannotriose (β-D-Glc (1→4) *versus* β-D-Man (1→4)) (Figure 1). Examination of protonated forms shows that only a slight mobility difference occurred between the linkage isomers (1→6 versus 1→4), with 0.997 V.s/cm^2 and 0.995 V.s/cm^2 for isomaltotriose and maltotriose, respectively (Figure 1a brown and blue trace, respectively). Varying α- to β- linkage, it reveals a significant shift from 0.995 V.s/cm^2 to 1.021 and 1.070 V.s/cm^2 for maltotriose to cellotriose, respectively (Figure 1a blue and green trace, respectively). The detection of two peaks, with similar abundance for cellotriose, can be putatively ascribed to either the presence of two equivalent protomers and/or to the co-existence of both α- and β-anomers. Using a different fully compositional isomer, one exhibits also a different mobility from 1.021/1.070 V.s/cm^2 to 1040 V.s/cm^2 for cellotriose to mannotriose, respectively (Figure 1a green and pink trace, respectively). In contrast to protonated forms, the ammoniated ones present a better difference like for isomalototriose/maltotriose couple with 1.034/1.006 V.s/cm^2 (Figure 1b, brown and blue trace, respectively), and for maltotriose/cellotriose one with 1.006/1.042 V.s/cm^2 (Figure 1b, blue and green trace, respectively). Mobility values were quasi similar for cellotriose/mannotriose one with 1.042/1.039 V.s/cm^2 (Figure 1b, green and pink trace, respectively) impairing any discrimination between us in such conditions. However, it was quoted out that with ammonium, only one peak is detected for the four carbohydrates even for cellotriose while two peaks were observed for protonated one. It seems to indicate that either only one ammonium attachment site exists or that an absence of interconversion occurrs during the course of

the experiment. Under sodiated forms, isomaltotriose shows two distinct peaks at 0.984 and 1.033 V.s/cm^2 but differing

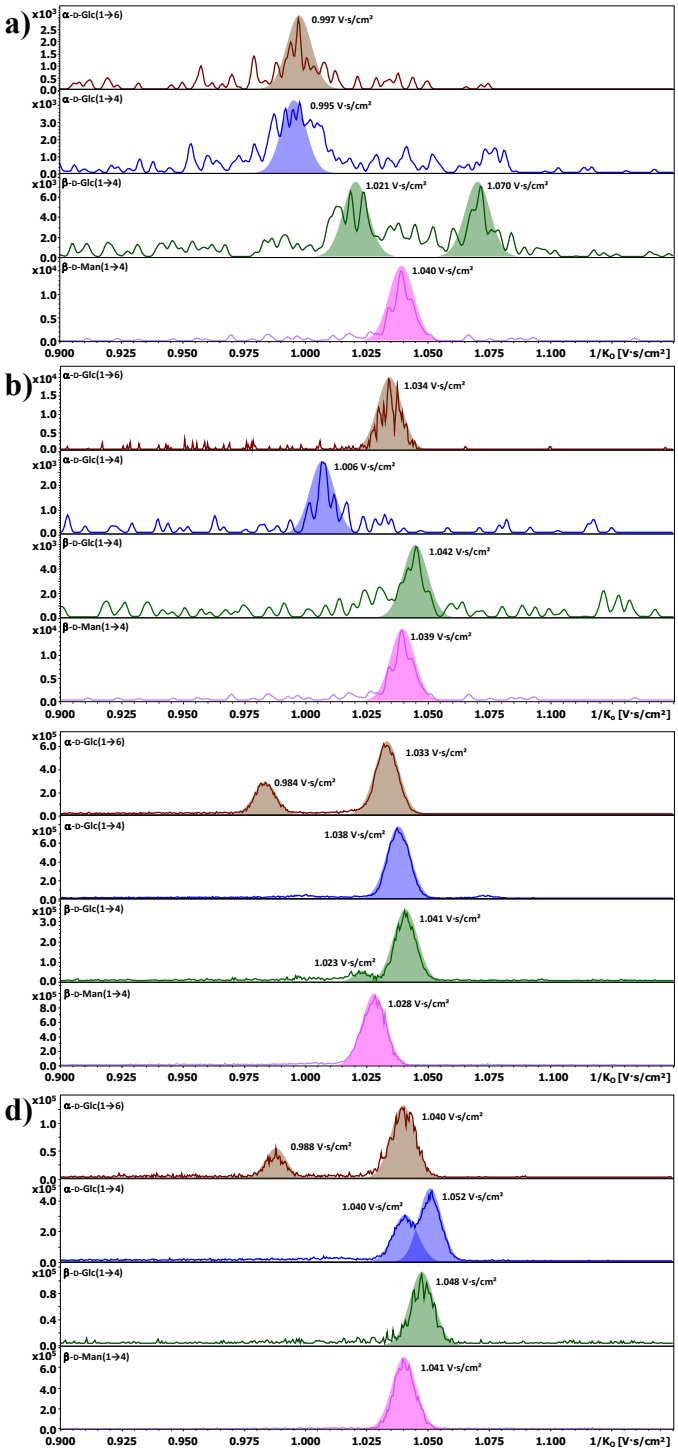

Figure 1. TIMS based mobilograms without any smoothing for trisaccharides showing difference in connectivity: α-D-Glc (1→6) *versus* (α-D-Glc (1→4) (isomaltotriose *versus* maltotriose),

anomery ((α-D-Glc (1→4) *versus* (β-D-Glc (1→4) (maltotriose *versus* cellotriose) and composition: β-D-Glc (1→4) *versus* β-D-Man (1→4) (cellotriose *versus* mannotriose) for a) singly protonated, b) singly sodiated, c) singly ammoniated and d) singly potassied trisaccharides. Measurement was achieved at a scan rate of 5.5 V/ms.

from the unique one recorded at 1.038 V.s/cm^2 for maltotriose (Figure 1c, brown and blue trace, respectively). This last one is very close from its β- anomer, cellotriose, with a mobility at 1.041 V.s/cm^2 (Figure 1c, green trace). Moreover, as for protonated form, a second but lower peak was detected at 1.023 V.s/cm^2. Sodiated mannotriose exhibits lower mobility shift (1.028 V.s/cm^2, Figure 1c, pink trace). Again with sodium, one can hypothesize that the observation of only one mobility peak from maltotriose and mannotriose may be attributed to its inability to mutarotate, and present two distinct α/β anomers at the OH group of C-1. The isomaltotriose and cellotriose both displayed two mobility features, presumably due to its α/β mutarotation, while maltotriose and mannotriose only displayed one such feature, perhaps due to the influence of the composition or linkage on mutarotation, and leading to a preference for only a single α or β anomer. Nonetheless, at this stage, it cannot be completely excluded that the two mobility peaks observed for isomaltotriose and cellotriose would result from different sodium attachment locations. As regards potassied forms, similar behaviour than for sodiated ones were obtained but with higher mobility values. However, two exceptions were highlighted for maltotriose and cellotriose. For the former, two unresolved peaks were detected at 1.040 V.s/cm^2 and 1.052 V.s/cm^2 (Figure 1d, blue trace) instead of only one with sodium (Figure 1c, blue trace). For the latter, only one peak was detected at 1.048 V.s/cm^2 (Figure 1d, green trace), instead of two with sodium (Figure 1c, green trace). Taking into account the results obtained for all trisaccharides (Table 1 and Figure 1), some general trends can be drawn where non-reducing trisaccharides (raffinose, melezitose, 1-kestose, gentianose, inulotriose, erlose) were higher in mobility, i.e. smaller in collision cross section or more compact in nature than the reducing ones (maltotriose, isomaltotriose, panose,

cellotriose, laminaritriose, mannotriose, 4'galactosyllactose). Additionally, the former exhibits only one mobility peak, and thus as speculated above, we have reasonably attributed this observation to a 'locked' configuration at the anomeric carbon, while the latter i.e. their reducible counterparts lead to two mobility peaks, potentially from α/β anomeric configurations as previously suggested (Nagy et al., 2018). However, it must keep in mind that the coexistence of multiple cation attachment sites or impurities at traces level can also exist and that may explain the results of sodiated and potassied gentianose as well as potassied inulotriose. Moreover, for a given monosaccharide composition, comparison of α *versus* β linked trisaccharides reveals that the β linked was more elongated (higher inverse reduced mobility i.e. lower mobility) than the α-linked (lower inverse reduced mobility i.e. higher mobility). In summary, TIMS experiments achieved until now at a defined scan rate (*Sr*) of 5.5 V/ms, and taking into account the type of adduct, compositional isomers, regioisomers and anomers, can be distinguished readily from each other on the basis of their elution voltage converted to ion mobility values and calculated CCS. Herein CSS values are in good agreement with some previously reported in literature (Table S1).

3.2 Enhancing isomers separations by adjusting ion mobility resolution.

The diminishment of *Sr,* aiming to reduce/avoid excessive ion mobility peak overlapping, significantly increases the mobility resolving power by ≈ 1.7 to 4 fold. As example, for singly potassied 4'galactosyllactose, *Sr* adjusted from 5.5 V/ms to 0.6 V/ms followed by 0.3 V/ms as the lowest scan value, led to high mobility resolving power (R ~ 87/92, 150/153 to 175/183, respectively) (Figure 2a). Even if the presence of two peaks issued from potassied 4'galactosyllactose was already distinguishable at *Sr* = 5.5 V/ms, lowering *Sr* offers a substantial enhancement of mobility resolution leading to a partial and almost complete baseline resolution

with r = 0.7, 1.0 and 1.3, respectively. Conversely, in the case of sodiated inulotriose only one large peak was initially detected. Varying *Sr* led to a significant increase of the mobility resolving power as well as R ~ 66, 133-170 and 137-226, for *Sr* 5.5, 0.6 and 0.3 V/ms, respectively.

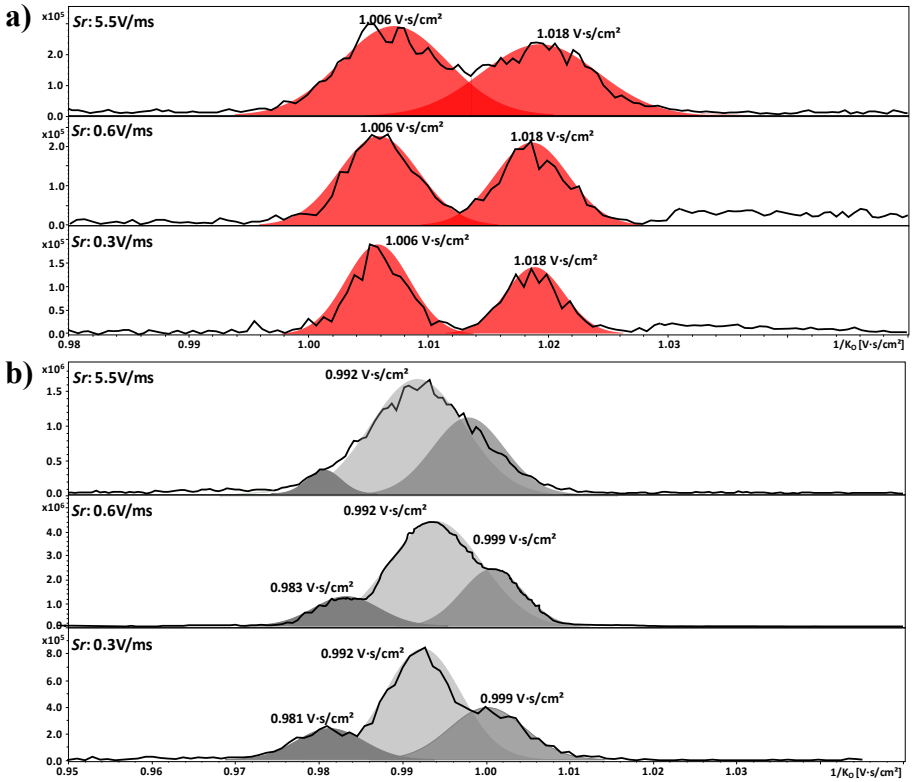

Figure 2. TIMS based mobilograms showing the influence of the scan ratio (*Sr*) from 5.5 V/ms to 0.3V/ms on both the resolving power (R) and resolution (r) for a) singly potassied 4'galactosyllactose and b) singly sodiated inulotriose.

It has thus permitted to highlight the presence of three different forms (Figure 2b). Such enhancement resulted in a possible mobility resolution r = 0.5 for peak 1/2 at *Sr* = 0.6 V/ms, which is slightly improved with r =0.7 and 0.6 for peak 1/2 and 2/3, respectively, at *Sr* = 0.3 V/ms. However, it was quoted out that each diminishment of *Sr* yields also to a slightly and gradual loss of sensitivity.

3.4 Identification and estimation of relative trisaccharides content in honeys.

Nowadays, traceability of foodstuff is of prime importance to ensure the highest level of consumer protection. Products must fulfil the criteria of quality that, day by day, are becoming more and more specific and exigent. Implemented detection and quantification methods are mainly based on chromatography. They are continuously improved to address the more and more restrictive quality rules of food industry, requiring the highest sensitivity. Such analytical methods should afford to reveal the conformity of the products, especially as regards possible contamination or adulteration, which can be hazardous to health or bias the real nutritional value. Honey is one of the most complex mixture of carbohydrates produced in nature and represents a good example since it is subject to these same demands. Literature reports that carbohydrate content of natural honey is mainly composed of monosaccharides (essentially glucose and fructose), disaccharides and trisaccharides at a level of 50-70%, 15-35% and 2-10%, respectively (Sanz et al., 2005). Presence of several oligosaccharides, portray only minority of the whole carbohydrates content, but can constitute a fingerprint indexing the honey authenticity and floral origin. Furthermore, examination of literature showed that if mono- and disaccharides content are the mainly studied carbohydrates during honeys analysis, trisaccharides have potential to be finer discriminating factor (Kaškonienė, V. & Venskutonis, P. R. 2010). Our TIMS approach was applied to reveal, identify and gain relative content of trisaccharides in honeys. As example, a forest based honey was infused and analysed by TIMS using a *Sr* of 0.6 V/ms. Resulting mobilogram showed two intense partially resolved peaks at $1/K_0$ = 0.982 and 0.999 V.s/cm^2 and one with a lower abundance but with a very large mobility range distribution, mainly unresolved, centred around 1.025 V.s/cm^2 (Figure 3a, top mobilogram). It can be also quoted out that the mobility range from 0.965 to 1.055 V.s/cm^2, ascribed to all detected peaks from honey, can theo-

retically correspond to twelve among the thirteen studied trisaccharides herein. A comparative GC-MS analysis was achieved, where 7 trisaccharides were identified among them i.e. raffinose, 1-kestose, erlose, melezitose, maltotriose, panose and isomaltotriose (Figure S2). A mixture containing these seven standard trisaccharides at 10µM (Mix dp3, see experimental section) was prepared. The mobilogram of Mixdp3 unambiguously confirms the presence of melezitose and 1-kestose ascribed to the two predominant peaks observed by ion mobility. Erlose can also be extracted from

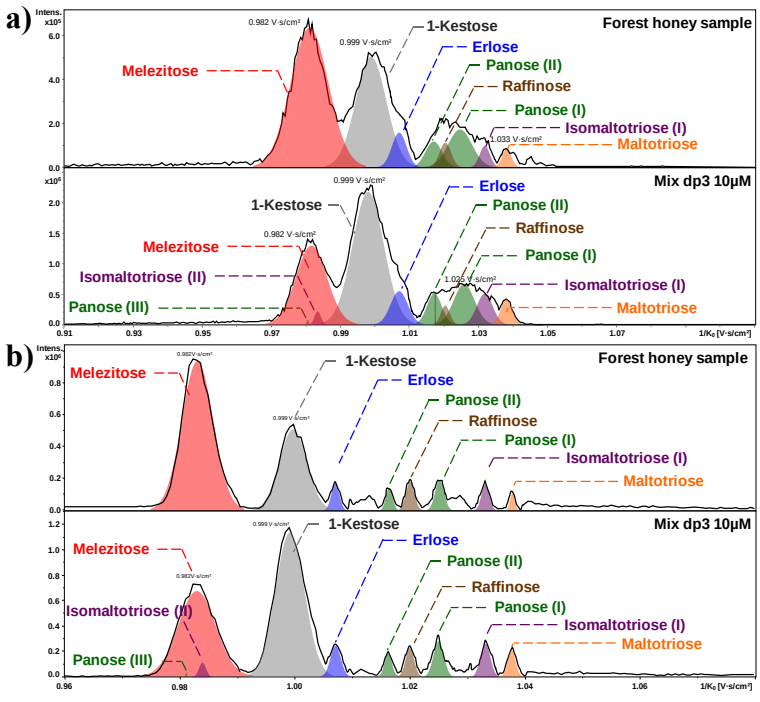

Figure 3. TIMS based mobilogram of the various singly sodiated trisaccharides ions of both standard mixture (top) and forest honey (below) acquired with the scan ratio of a) 0.6 V/ms and b) 0.3 V/ms.

the abnormal peak tailing of 1-Kestose peak. The deconvolution of the large mobility distribution in the 1.012-1.042 V.s/cm^2 range allows the putative assignment of panose, raffinose, isomaltotriose and maltotriose (Figure 3a, below mobilogram). For melezitose, 1-kestose/erlose and maltotriose, the resolving power (*R*) is 84, 69 and 201, respectively, while the unresolved peak of the

403 set constituted of panose, raffinose and isomaltotriose is only 54. As regards resolution (*r*), val-
404 ues of 0.77, 0.80 and 0.77 for melezitose to 1-kestose/erlose, 1-kestose/erlose to unresolved set
405 and unresolved set to maltotriose, respectively, were obtained. Nonetheless, it appears clearly
406 that a complete mobility resolution is a mandatory condition to fully address the unambiguous
407 and straightforward identification of the carbohydrates in crude samples. To reach that, a *Sr* of
408 0.3 V/ms was applied leading to a substantial improvement of both resolving power and mobility
409 resolution with a close baseline resolution for every compounds (Figure 3b). Specifically, with
410 such settings, erlose trace can be easily discriminated from 1-kestose, as well as the full set of
411 panose, raffinose, isomaltotriose and maltotriose. Using lower scan rates yields to clear im-
412 provement in both *R* and *r* with all values included in the range 126-722 and 1.15-2.19, respec-
413 tively. It contrasts with results obtained elsewhere as raffinose, isomaltotriose, melezitose and
414 maltotriose were not separated under $[M+Na]^+$ and were hardly resolved with a maximal r =
415 0.25, 0.52, 1.42, 0.27, 1.15 and 0.87 for maltotriose-isomaltotriose, maltotriose-raffinose, malto-
416 triose-melezitose, isomaltotriose-raffinose, isomaltotriose-melezitose and raffinose-melezitose
417 couple, respectively (Xie et al., 2020). Our GC-MS analysis showed similar profile to those pre-
418 viously observed by Sanz et al. (Sanz, M.L., Sanz, J., & Martínez-Castro, I. (2004) and de la
419 Fuente et al. (2011) as regards elution order and observation of possible *Z* and *E* isomers for mal-
420 totriose, isomaltotriose and panose (Figure S2). Nonetheless, several peaks for aforementioned
421 trisaccharides are also systematically observed without any derivatization (Figure 3 and Table 1).
422 Such results suggest that configurational isomers pre-exist before derivatization due to α/β mu-
423 tarotation, as evocated in section 3.1. Moreover, our TIMS approach overcomes frequent co-
424 elution problems observed with non-polar GC columns, especially between raffinose and kesto-
425 ses that may lead to misestimation (Sanz, M.L., Sanz, J., & Martínez-Castro, I., 2004; Ruiz-

Matute et al., 2010; de la Fuente et al., 2011). All *R* and *r* metrics are listed in Table S2. Interestingly, beyond only qualitative determination (identification criterion), one can access to a relative quantification (relative content criterion), providing to take into account the variation in response factor due to various ionization efficiency by comparing signals from independent analysis of the molecules alone or in mixture. Therefore, area integration allows establishing the relative content of the honeys as regards the seven trisaccharides. In this sense, TIMS approach reveals a similar abundance order both with *Sr* = 0.6 and 0.3 V/ms as follows: melezitose (28.2-28.3%) > raffinose (20.8-21.4%) > panose (13.7%) > erlose (12.2-12.6%) > 1-kestose (10.5-10.8%) > maltotriose (8.4-8.5%) > isomaltotriose (5.1-5.7%). Such content matched very well with those obtained by GC-MS analysis (Table 2). Both nature and relative abundance of trisaccharides can represent a potential signature of the floral sources (Cotte et al., 2003; Kaškonienė & Venskutonis, 2010). The data obtained for the seven carbohydrates and from the five honeys (Table S3) were analyzed in a one-way ANOVA. Results ported that all overall ANOVA *p*-value are smaller than 0.05 (95% confidence interval), hence at least two of the five honey have significantly different means whatever the given trisaccharides. Further statistical treatment by using Tukey test, i.e. mean comparisons, reveals further information regarding relationships between honeys (Table S4 and Figure S3).

445 **Table 2**. Relative content of the seven positively identified trisaccharides according to both the
446 two-based TIMS scan ratio (*Sr*) and GC-MS for the forest honey.

Identified trisaccharides	Relative content (%) (n=10)		
	Sr setting		GC-MS
	0.6 V/ms	0.3 V/ms	
1-Kestose	10.8 ± 1.4	10.5 ± 1.6	10.6 ± 2.3
Erlose	12.2 ± 0.5	12.6 ± 0.5	12.4 ± 1.5
Isomaltotriose	5.1 ± 0.7	5.7 ± 0.5	5.5 ± 1.2
Maltotriose	8.5 ± 0.5	8.4 ± 0.5	8.1 ± 1.4
Melezitose	28.2 ± 2.4	28.5 ± 2.1	28.7 ± 2.6
Panose	13.7 ± 1.5	13.7 ± 1.6	13.6 ± 1.8
Raffinose	21.4 ± 2.1	20.6 ± 1.8	20.9 ± 2.3

447
448
449 All of honey seemed to be discriminated using at least two significant trisaccharides content. In
450 addition, it appears that all the targeted trisaccharides can be used to the distinction of acacia and
451 forest honeys on one hand and rosemary and forest honeys on the other hand. All the seven
452 trisaccharides regarding their more or less complementary balances of significant/non-significant
453 means as 2/8 (1-kestose, isomaltotriose, panose, raffinose), 3/7 (erlose) and 1/9 (maltotriose,
454 melezitose) could be chosen as a relevant role authenticity/floral marker. Standardized principal
455 component analysis can explain the 88.7% of total variance using the two first components,
456 reaching 100% through four first components. It can be observed that the first principal compo-
457 nent is mainly a function of melezitose and erlose. The second principal component is essentially
458 a function of maltotriose and panose (Figure 4). In summary, the most important relative weights
459 in the first component are both positive (melezitose) and negative (erlose), this may be inter-
460 preted as a general balance to serve as index of each honey. A similar behaviour was obtained for
461 the second component where weights are both positive (maltotriose) and negative (panose). Su-
462 perimposition of the botanical origins represented according to the two first components, leading

to the botanical origin coordinates, known as centroid, using the scores obtained for honeys against their botanical origin.

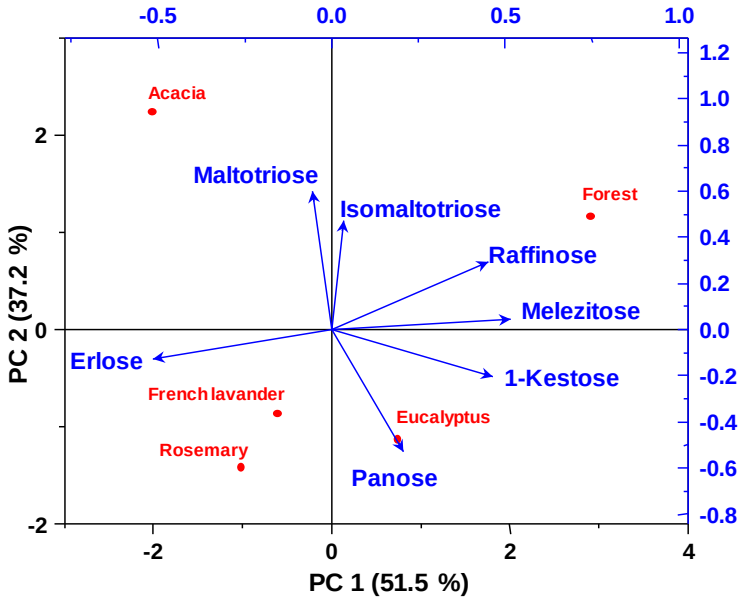

Figure 4. Superimposition of the representation of carbohydrates (blue) and of botanical origins (red) as a function of the two first principal components.

It may be seen that forest honey obtains the highest scores for the first component, while acacia and rosemary obtain the lowest. As such, the group of trisaccharides formed by melezitose, raffinose and erlose may play an important role in distinguishing among honeys of different botanical origins as observed in another study (Cotte et al. 2004). Acacia honey obtains higher scores in the second principal component than the remainder of botanical origins, above all relative to forest and much more to rosemary, eucalyptus and french lavender. Based on the two first principal components analysis and Tukey test, taking into account that all seven trisacharides were detected in the five honeys, we can suggest to use both abundance and ratio of trisaccharide as discriminant factor. For example, the herein honeys can be characterized with carbohydrates balance: forest with ≥20% of melezitose and ≥20% of melezitose/raffinose >1; acacia with malto-

triose >10%, panose <10% and erlose/maltotriose >4.5%; eucalyptus with panose >15%; 1-kestose >5% and panose /1-kestose >2%; french lavender with maltotriose >5%, panose >10% and erlose/maltotriose > 9%; rosemary with maltotriose <5%, panose >10% and erlose/maltotriose >9.5%. Such factors given to depict possible discriminative tree, need to be used with many precautions, since only a restricted set of honeys was assessed. Such approach should be further enriched with both a larger panel of honeys and other potential but very rare trisaccharides such as neo-kestose, 6-kestose, planteose or also theanderose. Another strategy holds in the introduction of canonical discriminant (Nozal et al., 2005), as a potential key to achieve a straightforward honeys classification, but the judicious choice of the suitable factor to considerate remains a delicate approach. Indeed, if single factors as presence and/or abundance of trisaccharides can be very effective to characterize the differences among monofloral honeys, that could be a more daunting task with honeys generically classified as multifloral. Moreover, the ratio between some mono-, di- or trisaccharides such as for example fructose/glucose, maltose/isomaltose, sucrose/turanose, and maltose/turanose or also maltotriose/(raffinose + erlose + melezitose) is another indicator that may be used to ascertain honey authenticity (Nozal et al., 2005). For example, an acacia honey was distinguished by a high maltose/isomaltose ratio (11:1 to 25:9), while this ratio for linden and honeydew honeys was remarkably lower, 2.2 and 2.0-2.5, respectively (Molnár-Perl & Horváth, 1997). A similar strategy was successfully used by Cotte et al. (2003) regarding maltotriose/trisaccharides ratio to distinguish various lavender honey.

4. CONCLUSIONS

We demonstrate in this work that the fast and direct analysis by TIMS represents a powerful and suitable alternative to longer chromatographic run, with analysis time of few minutes to more than one hour, respectively, to distinguish between 13 isomeric trisaccharides. Our IM strategy

has been successfully applied to 5 honeys, which are traditionally classified by time-consuming and high levels of expertise requiring pollen analyses. Our TIMS method tackles these aforementioned bottlenecks, by introducing an orthogonal strategy using 2 parameters i.e. *m/z* and CCS. After both optimization of TIMS resolution and determination of response factor due to various ionization efficiency, extraction of areas from IM afforded a straightforward relative quantification of trisaccharides in the honeys. Then, principal component analysis has been successfully employed as a first approach to characterize the 5 honeys, showing similarities or differences in trisaccharide content aiming to delineate potential floral markers. Moreover, *m/z* and CCS could be supplemented by upstream separation and MS/MS spectra to serve as additional dimensions. Ongoing expanding of this approach to operate at middle to high throughput, with or without other upstream separation methods, paves the way to the introduction of new routinely means in the field of glycomics.

ACKNOWLEDGMENTS

This work was supported by CEA and the French Ministry of Research and National Research Agency as part of the French metabolomics and fluxomics infrastructure (MetaboHUB, ANR-11-INBS-0010 grant).

REFERENCES

Ashline, D. J., Lapadula, A. J., Liu, Y.-H., Lin, M., Grace, M., Pramanik, B., & Reinhold, V. N. (2007). Carbohydrate Structural Isomers Analyzed by Sequential Mass Spectrometry. *Analytical Chemistry*, *79*, 3830‑3842. https://doi.org/10.1021/ac062383a.

Ben Faleh, A., Warnke, S., & Rizzo, T. R. (2019). Combining Ultrahigh-Resolution Ion-Mobility Spectrometry with Cryogenic Infrared Spectroscopy for the Analysis of Glycan Mixtures. *Analytical Chemistry*, *91*, 4876‑4882. https://doi.org/10.1021/acs.analchem.9b00659.

Carroll, J. A., Willard, D., & Lebrilla, C. B. (1995). Energetics of cross-ring cleavages and their relevance to the linkage determination of oligosaccharides. *Analytica Chimica Acta*, *307*, 431‐447. https://doi.org/10.1016/0003-2670(94)00514-M.

Clowers, B. H., Dwivedi, P., Steiner, W. E., Hill, H. H., & Bendiak, B. (2005). Separation of sodiated isobaric disaccharides and trisaccharides using electrospray ionization-atmospheric pressure ion mobility-time of flight mass spectrometry. *Journal of the American Society for Mass Spectrometry*, *16*, 660‐669. https://doi.org/10.1016/j.jasms.2005.01.010.

Cotte, J. F., Casabianca, H., Chardon, S., Lheritier, J., & Grenier-Loustalot, M. F. (2003). Application of carbohydrate analysis to verify honey authenticity. *Journal of Chromatography A*, *1021*, 145‐155. https://doi.org/10.1016/j.chroma.2003.09.005.

Cotte, J. F., Casabianca, H., Chardon, S., Lheritier, J., & Grenier-Loustalot, M. F. (2004). Chromatographic analysis of sugars applied to the characterisation of monofloral honey. *Analytical and Bioanalytical Chemistry*, *380*, 698-705. https://doi.org/10.1007/s00216-004-2764-1.de la Fuente, E., Ruiz-Matute, A.I., Valencia-Barrera, R.M., Sanz J., Martínez Castro I. (2011). Carbohydrate composition of Spanish unifloral honeys. Food Chemistry, 129, 1483–1489

Dell, A., & Morris, H. R. (2001). Glycoprotein Structure Determination by Mass Spectrometry. *Science*, *291*, 2351. https://doi.org/10.1126/science.1058890.

Duus, J. Ø., Gotfredsen, C. H., & Bock, K. (2000). Carbohydrate Structural Determination by NMR Spectroscopy : Modern Methods and Limitations. *Chemical Reviews*, *100*, 4589‐4614. https://doi.org/10.1021/cr990302n.

EGSF and IBCarb Network & European Science Foundation. (2014). *A Roadmap for Glycosciences in Europe.* (Vol. 1‐1). EGSF and IBCarb Network & European Science Foundation. A Roadmap for Glycosciences in Europe. http://ibcarb.com/wp-content/uploads/A-roadmap-for-Glycoscience-in-Europe.pdf. 2014. http://ibcarb.com/wp-content/uploads/A-roadmap-for-Glycoscience-in-Europe.pdf.

Gabryelski, W., & Froese, K. L. (2003). Rapid and sensitive differentiation of anomers, linkage, and position isomers of disaccharides using High-Field Asymmetric Waveform Ion Mobility Spectrometry

(FAIMS). *Journal of The American Society for Mass Spectrometry*, *14*, 265‐277. https://doi.org/10.1016/S1044-0305(03)00002-3.

Gaye, M. M., Kurulugama, R., & Clemmer, D. E. (2015). Investigating carbohydrate isomers by IMS-CID-IMS-MS: precursor and fragment ion cross-sections. *Analyst*, *140*, 6922‐6932. https://doi.org/10.1039/C5AN00840A.

Gaye, M. M., Nagy, G., Clemmer, D. E., & Pohl, N. L. B. (2016). Multidimensional Analysis of 16 Glucose Isomers by Ion Mobility Spectrometry. *Analytical Chemistry*, *88*, 2335‐2344. https://doi.org/10.1021/acs.analchem.5b04280.

Gray, C. J., Schindler, B., Migas, L. G., Pičmanová, M., Allouche, A. R., Green, A. P., Mandal, S., Motawia, M. S., Sánchez-Pérez, R., Bjarnholt, N., Møller, B. L., Rijs, A. M., Barran, P. E., Compagnon, I., Eyers, C. E., & Flitsch, S. L. (2017). Bottom-Up Elucidation of Glycosidic Bond Stereochemistry. *Analytical Chemistry*, *89*, 4540‐4549. https://doi.org/10.1021/acs.analchem.6b04998.

Harvey, D. J., Seabright, G. E., Vasiljevic, S., Crispin, M., & Struwe, W. B. (2018). Isomer Information from Ion Mobility Separation of High-Mannose Glycan Fragments. *Journal of the American Society for Mass Spectrometry*, *29*, 972‐988. https://doi.org/10.1021/jasms.8b05810.

Hofmann, J., Hahm, H. S., Seeberger, P. H., & Pagel, K. (2015). Identification of carbohydrate anomers using ion mobility–mass spectrometry. *Nature*, *526*, 241‐244. https://doi.org/10.1038/nature15388.

Hofmann, J., & Pagel, K. (2017). Glycan Analysis by Ion Mobility–Mass Spectrometry. *Angewandte Chemie International Edition*, *56*, 8342‐8349. https://doi.org/10.1002/anie.201701309.

Huang, Y., & Dodds, E. D. (2013). Ion Mobility Studies of Carbohydrates as Group I Adducts : Isomer Specific Collisional Cross Section Dependence on Metal Ion Radius. *Analytical Chemistry*, *85*, 9728‐9735. https://doi.org/10.1021/ac402133f.

Huang, Y., & Dodds, E. D. (2015). Discrimination of Isomeric Carbohydrates as the Electron Transfer Products of Group II Cation Adducts by Ion Mobility Spectrometry and Tandem Mass Spectrometry. *Analytical Chemistry*, *87*, 5664‐5668. https://doi.org/10.1021/acs.analchem.5b00759.

584 Kaškonienė, V., & Venskutonis, P. R. (2010). Floral Markers in Honey of Various Botanical and Geographic
585 Origins : A Review. *Comprehensive Reviews in Food Science and Food Safety*, *9*, 620‐ 634.
586 https://doi.org/10.1111/j.1541-4337.2010.00130.x.
587 Laine, R. A. (1994). Invited Commentary : A calculation of all possible oligosaccharide isomers both branched
588 and linear yields 1.05 × 1012 structures for a reducing hexasaccharide : The Isomer Barrier to devel-
589 opment of single-method saccharide sequencing or synthesis systems. *Glycobiology*, *4*, 759‐ 767.
590 https://doi.org/10.1093/glycob/4.6.759.
591 Lareau, N. M., May, J. C., & McLean, J. A. (2015). Non-derivatized glycan analysis by reverse phase liquid
592 chromatography and ion mobility-mass spectrometry. *Analyst*, *140*, 3335‐ 3338.
593 https://doi.org/10.1039/C5AN00152H.
594 Larriba, C., & Hogan, C. J. (2013). Ion Mobilities in Diatomic Gases : Measurement versus Prediction with
595 Non-Specular Scattering Models. *The Journal of Physical Chemistry A*, *117*, 3887‐ 3901.
596 https://doi.org/10.1021/jp312432z.
597 Marth, J. D. (2008). A unified vision of the building blocks of life. *Nature Cell Biology*, *10*, 1015‐ 1015.
598 https://doi.org/10.1038/ncb0908-1015.
599 McKenna, K. R., Li, L., Baker, A. G., Ujma, J., Krishnamurthy, R., Liotta, C. L., & Fernández, F. M. (2019).
600 Carbohydrate isomer resolution via multi-site derivatization cyclic ion mobility-mass spectrometry.
601 *Analyst*, *144*, 7220‐ 7226. https://doi.org/10.1039/C9AN01584A.
602 Molnár-Perl, I., & Horváth, K. (1997). Simultaneous quantitation of mono-, di-and trisaccharides as their TMS
603 ether oxime derivatives by GC-MS: I. In model solutions. *Chromatographia*, *45*, 321‐ 327.
604 https://doi.org/10.1007/BF02505578.
605 Mucha, E., González Flórez, A. I., Marianski, M., Thomas, D. A., Hoffmann, W., Struwe, W. B., Hahm, H. S.,
606 Gewinner, S., Schöllkopf, W., Seeberger, P. H., von Helden, G., & Pagel, K. (2017). Glycan Finger-
607 printing via Cold-Ion Infrared Spectroscopy. *Angewandte Chemie International Edition*, *56*,
608 11248‐ 11251. https://doi.org/10.1002/anie.201702896.
609 Nagy, G., Attah, I. K., Garimella, S. V. B., Tang, K., Ibrahim, Y. M., Baker, E. S., & Smith, R. D. (2018).
610 Unraveling the isomeric heterogeneity of glycans : Ion mobility separations in structures for lossless

ion manipulations. *Chemical Communication*, *54*, 11701- 11704. https://doi.org/10.1039/C8CC06966B.

National Research Council (US). (2012). *Committee on Assessing the Importance and Impact of Glycomics and Glycosciences. Trans-forming Glycoscience A Roadmap for the Future*. National Academies Press. ttps://www.ncbi.nlm.nih.gov/books/NBK109958/pdf/Bookshelf_NBK109958.pdf.

Nozal, M. J., Bernal, J. L., Toribio, L., Alamo, M., Diego, J. C., & Tapia, J. (2005). The Use of Carbohydrate Profiles and Chemometrics in the Characterization of Natural Honeys of Identical Geographical Origin. *Journal of Agricultural and Food Chemistry*, *53*, 3095- 3100. https://doi.org/10.1021/jf0489724.

Paglia, G., Williams, J. P., Menikarachchi, L., Thompson, J. W., Tyldesley-Worster, R., Halldórsson, S., Rolfsson, O., Moseley, A., Grant, D., Langridge, J., Palsson, B. O., & Astarita, G. (2014). Ion Mobility Derived Collision Cross Sections to Support Metabolomics Applications. *Analytical Chemistry*, *86*, 3985- 3993. https://doi.org/10.1021/ac500405x.

Pu, Y., Ridgeway, M. E., Glaskin, R. S., Park, M. A., Costello, C. E., & Lin, C. (2016). Separation and Identification of Isomeric Glycans by Selected Accumulation-Trapped Ion Mobility Spectrometry-Electron Activated Dissociation Tandem Mass Spectrometry. *Analytical Chemistry*, *88*, 3440- 3443. https://doi.org/10.1021/acs.analchem.6b00041.

Riggs, D. L., Hofmann, J., Hahm, H. S., Seeberger, P. H., Pagel, K., & Julian, R. R. (2018). Glycan Isomer Identification Using Ultraviolet Photodissociation Initiated Radical Chemistry. *Analytical Chemistry*, *90*, 11581- 11588. https://doi.org/10.1021/acs.analchem.8b02958.

Ruiz-Matute A.I., Brokl M., Soria A.C., Sanz M.L., Martínez-Castro I. (2010) Gas chromatographic–mass spectrometric characterisation of tri- and tetrasaccharides in honey. *Food Chemistry, 120*, 637-642. https://doi.org/10.1016/j.foodchem.2009.10.050.

Sanz, M.L., Polemis, N., Morales, V., Corzo, N., Drakoularakou, A., Gibson, G. R., & Rastall, R. A. (2005). In Vitro Investigation into the Potential Prebiotic Activity of Honey Oligosaccharides. *Journal of Agricultural and Food Chemistry*, *53*, 2914- 2921. https://doi.org/10.1021/jf0500684.

Sanz, M.L., Sanz, J., & Martínez-Castro, I. (2004). Gas chromatographic–mass spectrometric method for the qualitative and quantitative determination of disaccharides and trisaccharides in honey. *Journal of Chromatography A*, *1059*, 143‐148. https://doi.org/10.1016/j.chroma.2004.09.095.

Schindler, B., Barnes, L., Renois, G., Gray, C., Chambert, S., Fort, S., Flitsch, S., Loison, C., Allouche, A.-R., & Compagnon, I. (2017). Anomeric memory of the glycosidic bond upon fragmentation and its consequences for carbohydrate sequencing. *Nature Communications*, *8*, 973. https://doi.org/10.1038/s41467-017-01179-y.

Schindler, B., Laloy-Borgna, G., Barnes, L., Allouche, A.-R., Bouju, E., Dugas, V., Demesmay, C., & Compagnon, I. (2018). Online Separation and Identification of Isomers Using Infrared Multiple Photon Dissociation Ion Spectroscopy Coupled to Liquid Chromatography : Application to the Analysis of Disaccharides Regio-Isomers and Monosaccharide Anomers. *Analytical Chemistry*, *90*, 11741‐11745. https://doi.org/10.1021/acs.analchem.8b02801.

Varki, A. (2015). *Essentials of Glycobiology* (3rd Ed., Vol. 1). Cold Spring Harbor Laboratory Press.

Wei, J., Wu, J., Tang, Y., Ridgeway, M. E., Park, M. A., Costello, C. E., Zaia, J., & Lin, C. (2019). Characterization and Quantification of Highly Sulfated Glycosaminoglycan Isomers by Gated-Trapped Ion Mobility Spectrometry Negative Electron Transfer Dissociation MS/MS. *Analytical Chemistry*, *91*, 2994‐3001. https://doi.org/10.1021/acs.analchem.8b05283.

Xie, C., Wu, Q., Zhang, S., Wang, C., Gao, W., Yu, J., & Tang, K. (2020). Improving glycan isomeric separation via metal ion incorporation for drift tube ion mobility-mass spectrometry. *Talanta*, *211*, 120719. https://doi.org/10.1016/j.talanta.2020.120719.

Zheng, X., Aly, N. A., Zhou, Y., Dupuis, K. T., Bilbao, A., Paurus, V. L., Orton, D. J., Wilson, R., Payne, S. H., Smith, R. D., & Baker, E. S. (2017). A structural examination and collision cross section database for over 500 metabolites and xenobiotics using drift tube ion mobility spectrometry. *Chemical Science*, *8*, 7724‐7736. https://doi.org/10.1039/C7SC03464D.

Zheng, X., Zhang, X., Schocker, N. S., Renslow, R. S., Orton, D. J., Khamsi, J., Ashmus, R. A., Almeida, I. C., Tang, K., Costello, C. E., Smith, R. D., Michael, K., & Baker, E. S. (2017). Enhancing glycan isomer separations with metal ions and positive and negative polarity ion mobility spectrometry-mass

663 spectrometry analyses. *Analytical and Bioanalytical Chemistry*, *409*, 467‐476.
664 https://doi.org/10.1007/s00216-016-9866-4.

665